How to Design a Passive Damped LCL Coupling Filter for an Active DC-Traction Substation

Mihaela Popescu, Alexandru Bitoleanu, Mircea Dobriceanu and Florin Alexandru Teodorescu

University of Craiova, Faculty of Electrical Engineering, Craiova, Romania

mpopescu@em.ucv.ro, alex.bitoleanu@em.ucv.ro, mdobriceanu@em.ucv.ro, ax.teodorescu@gmail.com

Abstract – **The attention in this paper is directed to the design of a passive damped LCL filter intended to connect the voltage source inverter of an active DC-traction substation to the AC-power supply. Based on the tasks to be fulfilled by the passive connecting filter related to the current filtering and its dynamics, the mathematical foundation of the LCL filter design consists in taking into consideration the transfer function of the currents, the switching frequency, the resonance frequency and the compensated harmonics by active filtering. A design algorithms is formulated, by considering the imposition of the attenuation corresponding to the switching frequency. Besides this, the position of the resonance frequency relative to the frequency of the highest order harmonic to be compensated is imposed. The design algorithm is fully formulated, and specific indicators are defined and used to evaluate the performance of the whole active filtering system. The case study taken into consideration is of the active DC-traction substation, where the uncontrolled traction rectifier is of 12-pulse parallel type. Based on Matlab-Simulink modeling, the simulation of the whole active DC-traction substation operating in both active filtering and regeneration regimes illustrates the proper behavior of the system and the influence of the LCL filter parameters on the power quality performance.**

Cuvinte cheie: tractiune in c.c., filtrare activa de putere, regenerare, filtru LCL, rezistenta de amortizare.

Keywords: *DC-traction, active power filtering, regeneration, LCL filter, damping resistance.*

I. INTRODUCTION

Two issues have been identified so far in the operation of the classical DC-traction substations with uncontrolled rectifiers, whose solving can lead to increased energy efficiency.

The former consists of the distorted current in the traction transformer primary due to the traction rectifier's operation during the traction regime. For instance, the total harmonic distortion (*THD*) factor of about 12% in the case of 12-pulse rectifier, and about 30% in the case of 6-pulse rectifier are common values [1]–[4], which do not meet the standards and recommendations for harmonic control, i.e. IEEE-519 [5]. The modern, flexible and high performance solution of adding a shunt active power filter (SAPF) based on voltage source inverter (VSI) structure in the point of common coupling (PCC) is the solution increasingly adopted to solve this problem [6]–[9].

The latter is related to the impossibility of sending back into the grid the energy resulting from the regenerative braking process of the traction motors, due to the unidirec-

tional traction rectifier. Besides the solution of the direct return to the AC-power supply [10]–[12], the new solution called "active substation" ensures both the recovering the surplus energy in the traction substation and the power factor compensation [13]–[15].

As the active traction substation involves the addition of a VSI acting as SAPF, the performance of the system depends on the circuits of connection and their design.

The use of the LCL passive filter to interface the inverter with the power grid is an increasingly common solution compared with the classical L filter, due to the smaller size and cost and better performance [16]–[18].

Regarding the tasks of a LCL filter connected at the output of VSI acting as SAPF, the specificity consists of the ability of reducing as much as possible the switching harmonics without modify the harmonics of low order to be compensated by active filtering. A compromise must be made in this respect.

In the design of the LCL filter, the use of transfer functions as admittances or impedance characteristics is often found in literature [8], [9]. In our opinion, due to the low-pass wideband behavior of the LCL filter against the current harmonics at the inverter output, the design information is obtained from the transfer function as the relationship of the LCL's output current to its input current [19]–[23].

In this paper, the design algorithm of the LCL filter with damping resistance is conceived based on the transfer function of the currents and imposing some specific quantities related to the filter's performance.

The paper is organized as follows. Section II briefly describes the active DC-traction substation. Then, the LCL filter tasks and transfer function are presented, followed by the performance indicators. The mathematical foundation and the design algorithm are the subject of Section V. The next section illustrates the simulation results for the practical case of an active DC-traction substation with 12-pulse parallel rectifier. The key findings are expressed in the end of the paper.

II. STRUCTURE OF THE ACTIVE DC-TRACTION SUBSTATION

The structure of the active DC-traction substation shown in Fig. 1 highlights the IGBT-based voltage source inverter as the key component added to the existing traction substation with uncontrolled rectifier. The LCL filter with damping resistance makes the connection with the recovery transformer which ensures the proper level of the VSI voltage on its AC-side [15], [19]–[23].
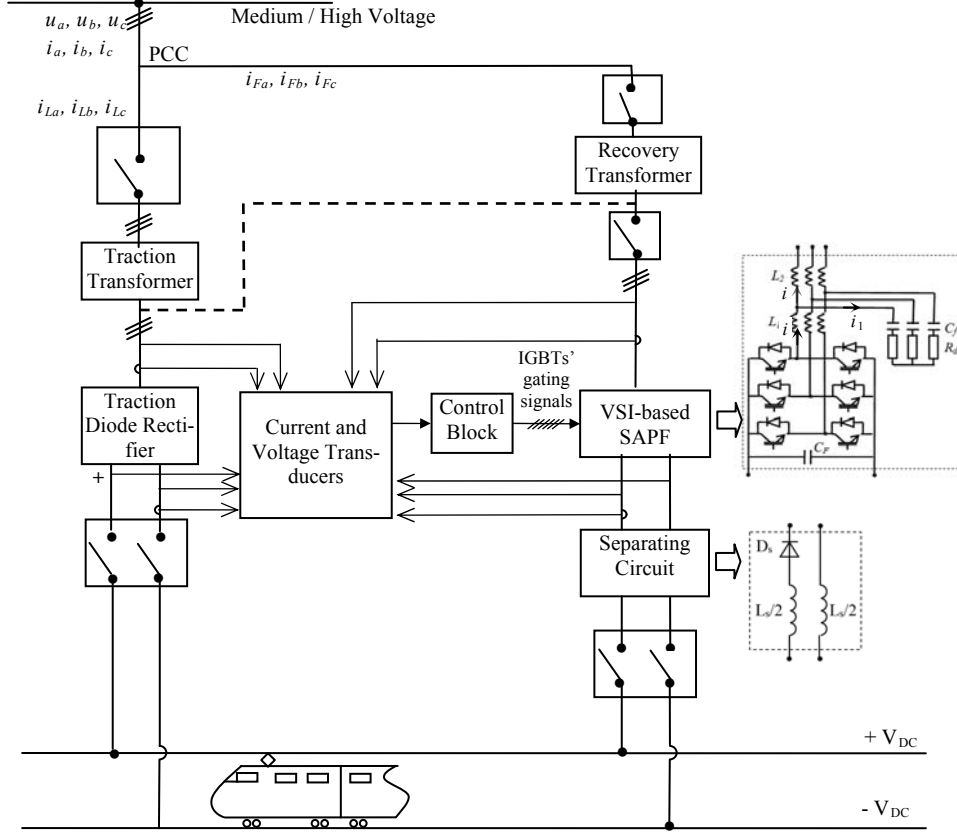
Fig. 1. DC-traction substation with active filtering and regeneration capabilities.

In the traction regime of the traction substation, the diode of the separating circuit on the DC-side is blocked and VSI acts as a shunt active filter improving the power quality on the AC-side.

When the traction motors operate in braking regime, the separating diode is forward biased and the associated regenerative energy is sent back into the power supply.

The AC-current provided by VSI is controlled in indirect mode, by handling the supply current upstream the point of common coupling (PCC) [24], [25].

III. LCL FILTER TASKS AND TRANSFER FUNCTION

The main tasks of the passive LCL filter on the AC-side of the VSI acting as SAPF are the following [23]:
 - rejecting the IGBTs' switching harmonics;
 - all harmonics to be compensated should pass unaltered, in order to obtain sinusoidal supply currents;
 - ensuring a good dynamics of the current, in accordance with the prescribed current.

The main transfer function of the LCL filter with damping resistors, which is very useful in the design procedure, is related to input and output currents [19], [20], [23] i.e.:

$$G_1(s) = I_2(s)/I_1(s) = \left(1 + sR_dC_f\right)\Big/\left(1 + sR_dC_f + s^2L_2C_f\right) \quad (1)$$

Thus, the associated expressions of the transfer function modulus and resonance frequency are [19], [21]-[23]:

$$|G_1(j\omega)|^2 = \frac{1 + \left(R_dC_f\right)^2\omega^2}{\left(1 - L_2C_f\omega^2\right)^2 + \left(R_dC_f\right)^2\omega^2}; \quad (2)$$

$$\omega_{res} = 1\big/R_dC_f \cdot \sqrt{\sqrt{\left(L_2C_f + 2R_d^2C_f^2\right)\Big/\left(L_2C_f\right)} - 1}. \quad (3)$$

As illustrated by (1), (2) and (3), only the pair of products L_2C_f and R_dC_f intervenes and, consequently, they can be determined based on some conditions related of attenuation and frequency.

IV. PERFORMANCE INDICATORS

Since the same values of the products L_2C_f and R_dC_f can be obtained from several sets of parameters L_2, C_f and R_d, the use of some performance indicators in the design algorithm is absolutely necessary.

The first one is related to the losses (P_d) on the damping resistors, which has the meaning of an equivalent resistance (R_{ech}) [19], [22]:

$$P_d\big/I_1^2 = R_{ech} = 3R_d\,\frac{(\omega_{sw}^2L_2C_f)^2}{(1 - \omega_{sw}^2L_2C_f)^2 + \omega_{sw}^2R_d^2C_f^2}\,, \quad (4)$$

where ω_{sw} is the switching frequency.

The second performance indicator gives information on the extent to which the presence of the interface filter influences the harmonics to be compensated, whose order is below N.

Three expressions are proposed to be used for this kind of indicator:

$$PI_1 = 1 - \sqrt{\sum_{k=1}^{N}\left(\left|G(\omega_k)\right| - 1\right)^2}; \quad (5)$$

$$PI_2 = 1 - \sqrt{\frac{\sum_{k=1}^{N}\left(|G(\omega_k)|-1\right)^2 k^2}{\sum_{k=1}^{N}k^2}} \ , \qquad (6)$$

$$PI_3 = 1 - \sqrt{\frac{\sum_{k=1}^{N}\left(|G(\omega_k)|-1\right)^2 / k^2}{\sum_{k=1}^{N}1/k^2}} \ , \qquad (7)$$

all them having values less than 1. The performance is all the better, as PI approaches the value of 1.

The indicator introduced by (5) treats equally each harmonic, the one corresponding to (6) penalizes the amplification of the harmonics close to fN, and the one corresponding to the (7) penalizes the amplification of the low order harmonics.

V. MATHEMATICAL FOUNDATION AND DESIGN ALGORITHM

The mathematical foundation of the design algorithm relies on the role of the LCL filter.

Thus, based on expression (2) of the square of the transfer function modulus, the condition of switching harmonics attenuation is expressed as:

$$\frac{1+\omega_{sw}^2 R_d^2 C_f^2}{(1-\omega_{sw}^2 L_2 C_f)^2 + \omega_{sw}^2 R_d^2 C_f^2} = m_{sw}^2 , \qquad (8)$$

where m_{sw} is the imposed magnitude response at the switching frequency.

As the behavior of the connecting filter depends on the resonance frequency ω_{res} compared to the frequency ω_N associated to the highest order harmonics to be compensated, the ratio q of these quantities will be introduced in the design algorithm,

$$q = \omega_{res}/\omega_N . \qquad (9)$$

Thus, expression (3) becomes:

$$\frac{1}{R_d C_f}\sqrt{\sqrt{\frac{L_2 C_f + 2R_d^2 C_f^2}{L_2 C_f}}-1} = q\omega_N . \qquad (10)$$

After processing (10), the square of the product $R_d C_f$ is expressed as follows:

$$R_d^2 C_f^2 = \frac{2\left(1 - q^2\omega_N^2 L_2 C_f\right)}{q^4 \omega_N^4 L_2 C_f} . \qquad (11)$$

Along with (8), expression (11) provides the second relationship between the products $L_2 C_f$ and $R_d C_f$.

After replacing (11) into (8), the following equation is obtained:

$$m_{sw}^2 q^4 z^4 \omega_N^6 \left(L_2 C_f\right)^3 - 2m_{sw}^2 q^4 z^2 \omega_N^4 \left(L_2 C_f\right)^2 + \\ + q^2\left(1-m_{sw}^2\right)\left(2z^2 - q^2\right)\omega_N^2 L_2 C_f - 2z^2\left(1-m_{sw}^2\right) = 0 \quad , \qquad (12)$$

which gives the product $L_2 C_f$ as a function of m_{sw}, q, ω_N, and ω_{sw} appearing in parameter z introduced to simplify the form of the equation,

$$z = \omega_{sw}/\omega_N . \qquad (13)$$

Then, the product $R_d C_f$ is provided by (11).

It should be noticed that, based on (11), there is a limitation related to product $L_2 C_f$, as follows:

$$L_2 C_f < \frac{1}{q^2\omega_N^2} . \qquad (14)$$

In the following analysis, the magnitude responses for frequencies ω_N and ω_{res} are taken into consideration too:

$$m_N = \sqrt{\frac{1+\omega_N^2 R_d^2 C_f^2}{(1-\omega_N^2 L_2 C_f)^2 + \omega_N^2 R_d^2 C_f^2}} ; \qquad (15)$$

$$m_{res} = \sqrt{\frac{1+\omega_{res}^2 R_d^2 C_f^2}{(1-\omega_{res}^2 L_2 C_f)^2 + \omega_{res}^2 R_d^2 C_f^2}} . \qquad (16)$$

Based on expressions (8), (11), (15) and (16) and taking into consideration condition (14), the dependencies of the magnitudes m_N, m_{sw} and m_{res} as functions of the products $L_2 C_f$ and $R_d C_f$ for different values of the parameter q are presented in figures from 2 to 5. The influence of $L_2 C_f$ on the performance indicators PI_1, PI_2 and PI_3 for N=31 is illustrated too.
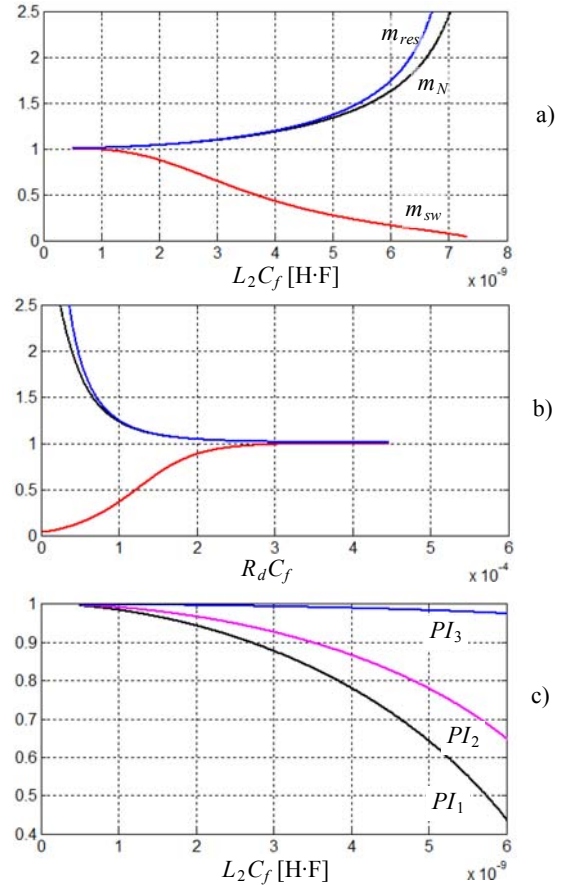

Fig. 2. Magnitudes m_N, m_{sw} and m_{res} as functions of $L_2 C_f$ (a) and $R_d C_f$ (b) and indicators PI_1, PI_2 and PI_3 as functions of $L_2 C_f$ (c), for q=1.2.
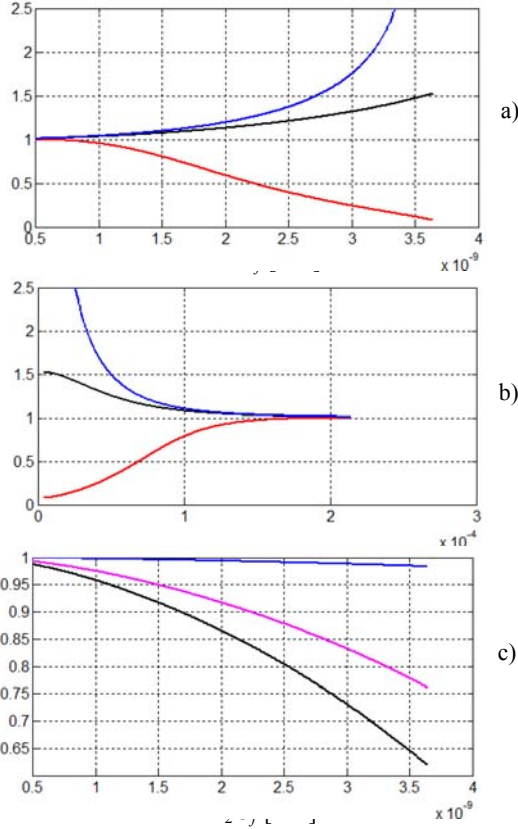
Fig. 3. Magnitudes m_N, m_{sw} and m_{res} as functions of L_2C_f (a) and R_dC_f (b) and indicators PI_1, PI_2 and PI_3 as functions of L_2C_f (c), for $q=1.7$.
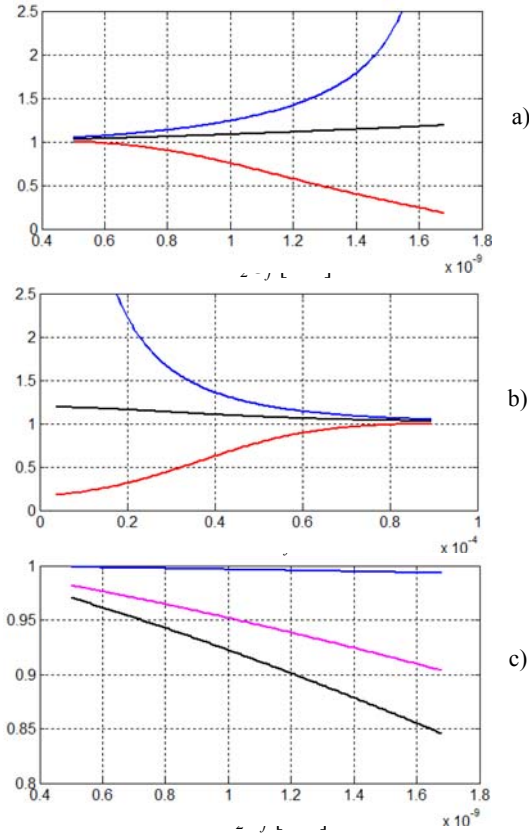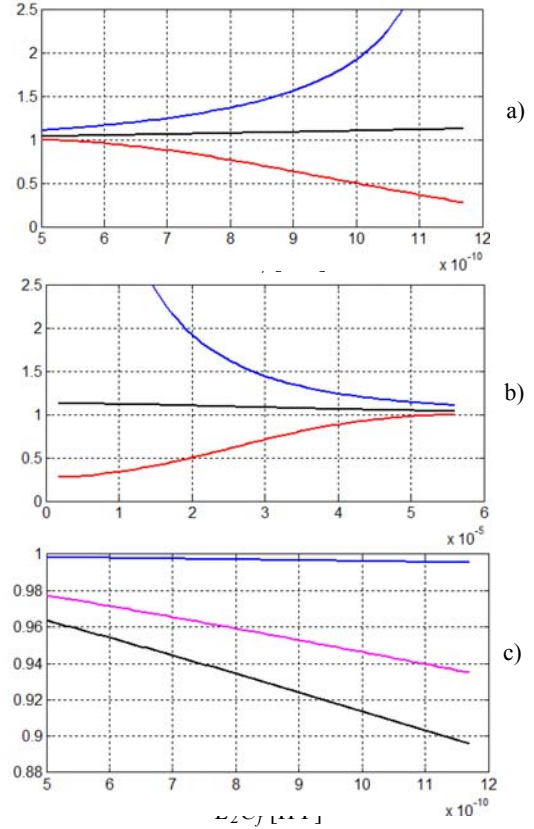

Fig. 5. Magnitudes m_N, m_{sw} and m_{res} as functions of L_2C_f (a) and R_dC_f (b) and indicators PI_1, PI_2 and PI_3 as functions of L_2C_f (c), for $q=3$.

It can be seen that the magnitude m_{sw} decreases as product L_2C_f increases and product R_dC_f decreases, and it is lower at lower values of q. On the other hand, both magnitudes m_N and m_{res} increase as L_2C_f increases and R_dC_f decreases, which is an unfavorable aspect. It means that a compromise between the very high attenuation of the switching harmonics and the very little influence on harmonics to be compensated must be adopted.

For instance, the highest value of L_2C_f for $q=1.7$ is $3.64·10^{-9}$ H·F and the associated value of R_dC_f is $4.055·10^{-6}$ Ω·F. In this case, m_{sw} is about 0.0772 (i.e. -22.25 dB), $m_N=1.53$, and $m_{res}=14.92$, as illustrated in Fig. 3 a) and b). By comparison, for the same q, but $L_2C_f=1.99·10^{-9}$ H·F, $R_dC_f=7.797·10^{-5}$ Ω·F, the performance in diminishing the switching harmonics is very poor, as $m_{sw}=0.59$, which means only -4.58 dB. As regards the amplification at frequency f_N, it is lower by 0.4 (1.13 compared to 1.53). The resonance magnitude m_{res} is diminished to an even greater extent (1.19 compared to 14.92).

Smaller amplification of the harmonics to be compensated by active filtering is obtained at higher values of parameter q. For example, when L_2C_f is the highest possible for $q=2.5$ ($L_2C_f=1.68·10^{-9}$ H·F), $m_N=1.18$, but m_{sw} is 0.18, which means -14.89 dB (Fig. 4), compared to -22.25 dB for $q=1.7$ (Fig. 3).

The influence of L_2C_f on the performance indicators PI_1, PI_2 and PI_3 which are related to m_N, for different values of q (Figs. 2, 3, 4 and 5 c)) confirm the previous conclusions. Thus, all three indicators, but especially PI_1 and PI_2, have better values at higher values of q. Unfortunately, the influence of the IGBTs' switching on the current is expected to remain rather high.

Fig. 4. Magnitudes m_N, m_{sw} and m_{res} as functions of L_2C_f (a) and R_dC_f (b) and indicators PI_1, PI_2 and PI_3 as functions of L_2C_f (c), for $q=2.5$.

Fig. 6 shows the relationship between products L_2C_f and R_dC_f for four values of q across the whole range of L_2C_f. As exhibited, the range of L_2C_f becomes narrower as q increases and the product R_dC_f decreases as the product L_2C_f increases, irrespective of the value of q.

When different values of the capacitance are taken into consideration to obtain the resulted products L_2C_f and R_dC_f in order to obtain the highest attenuation of the switching harmonics, Fig. 7 illustrates the needed values of the damping resistance R_d and inductance L_2. As shown, both quantities are smaller in the case of higher values of q. Quantitatively, the value of inductance is much more influenced by the value of q, especially for low values of the capacitance. As an example, for $C_f =1$ µF, L_2=3.64 mH if q=1.7 and L_2=1.68 mH if q=2.5.

The equivalent resistance, which gives information on the power losses on the damping resistance, is obviously higher for q=1.7, as this case corresponds to a greater attenuation of the switching harmonics (Fig. 8).

The Bode magnitude diagrams in Figs. 9 and 10 highlight better the behavior of the filter with respect to frequencies ω_N and ω_{sw}, as well as the resonance frequency.
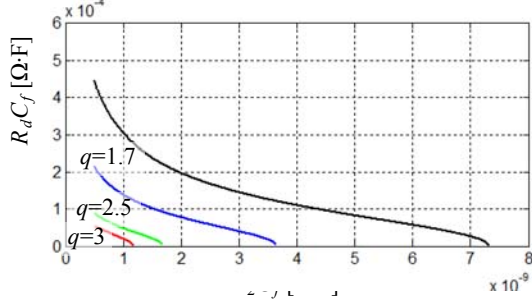
Fig. 6. R_dC_f as function of L_2C_f for different values of q.
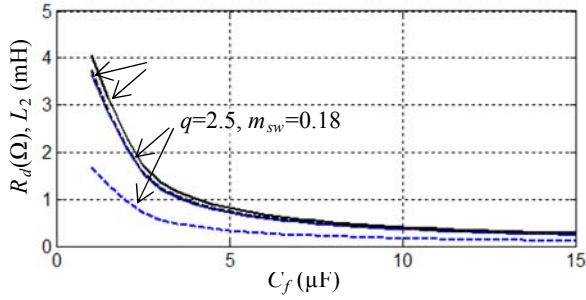
Fig. 7. R_d (in black) and L_2 (in blue) as function of C_f : for q=1.7 (continuous line) and q=2.5 (dashed line).
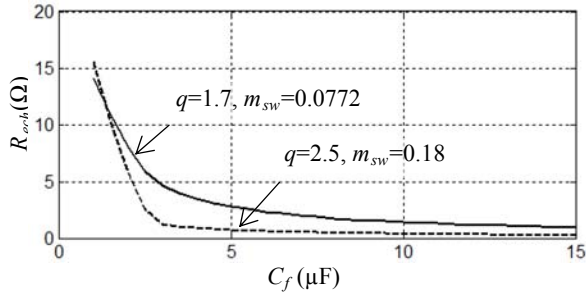

Fig. 8. R_{ech} as function of C_f : for q=1.7 (continuous line) and q=2.5 (dashed line).
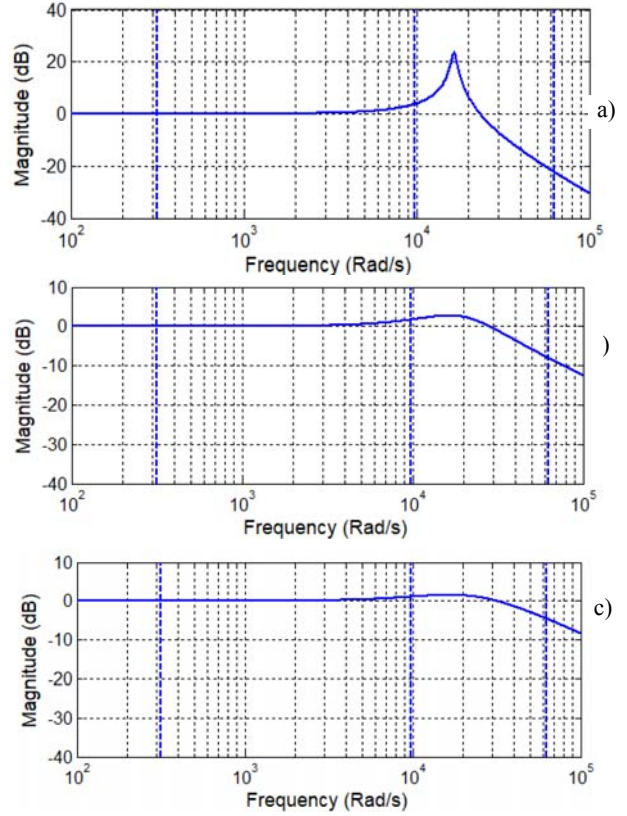

Fig. 9. Bode magnitude diagrams when q=1.7 and C_f =5µF, for: a) R_d =0.81 Ω, L_2=0.73 mH (m_{sw}=0.0772); b) R_d=11.65 Ω, L_2=0.5 mH (m_{sw}=0.397); c) R_d =15.6 Ω, L_2=0.39 mH (m_{sw}=0.593).
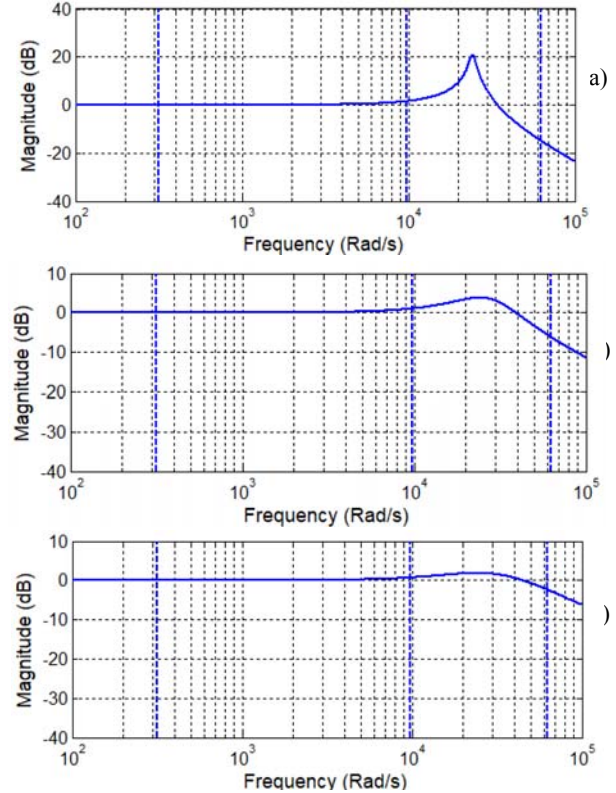
Fig. 10. Bode magnitude diagrams when q=2.5 and C_f =5µF, for: a) R_d =0.45 Ω, L_2=0.34 mH (m_{sw}=0.18); b) R_d=6.44 Ω, L_2=0.26 mH (m_{sw}=0.494); c) R_d =9.74 Ω, L_2=0.2 mH (m_{sw}=0.762).

The diagram in Fig. 9 a) corresponds to the highest attenuation at the switching frequency (m_{sw}=0.0772) for q=1.7 and C_f =5µF. The associated values of the performance indicators are: PI_1 = 0.612, PI_2 = 0.762, PI_3 = 0.983, R_{ech} = 2.81 Ω. The others diagrams in Fig. 9 show a lower magnification at frequency ω_N, leading to increased values of indicators PI, PI_2 and PI_3, but a lower attenuation at frequency ω_{sw}.

Similar aspects are exhibited by the Bode diagrams in Fig. 10 for q=2.5 and C_f =5µF. Even if the magnification at frequency ω_N is lower than in the case of q=1.7, the attenuation at frequency ω_{sw} is lower too.

Based on the previous mathematical foundation, the design algorithm was conceived and it is summarized in Fig. 11.

VI. SIMULATION RESULTS

In order to assess the behavior of the LCL filter designed by the algorithm above, a specific Matlab-Simulink model of an active DC-traction with 12-pulse parallel diode rectifier has been conceived. It contains:
- The traction transformer with Y/y/d connection, 2 MVA; 33 kV/ 1.2 kV/ 1.2 kV;
- The recovery transformer with Y/y connection, 2.2 MVA; 820 V/ 33 kV;
- The DC-traction line with rated voltage of 1500 V;
- The DC-coupling circuit, with C_F=100 mF and L_s=40 µH.

Three sets of values for the LCL filter with damping resistance, which are provided by the proposed design algorithm, are taken into consideration. They correspond to f_{sw}=10 kHz and N=31.
Set 1. C_f =5µF, R_d =0.81 Ω, L_2=0.73 mH, obtained for q=1.7 and m_{sw}=0.077;
Set 2. C_f =5µF, R_d =15.6 Ω, L_2=0.39 mH, obtained for q=1.7 and m_{sw}=0.593;
Set 3. C_f =15µF, R_d =0.25 Ω, L_2=0.11 mH, obtained for q=2.5 and m_{sw}=0.182.

As regards the inductance L_1 of the LCL filter, it does not influence the transfer function between output and input currents, so that a small value L_1=L_2/10 was taken into consideration, to limit the IGBTs' switching losses.

The operation of the active DC-traction substation in both traction and regeneration modes has been simulated.
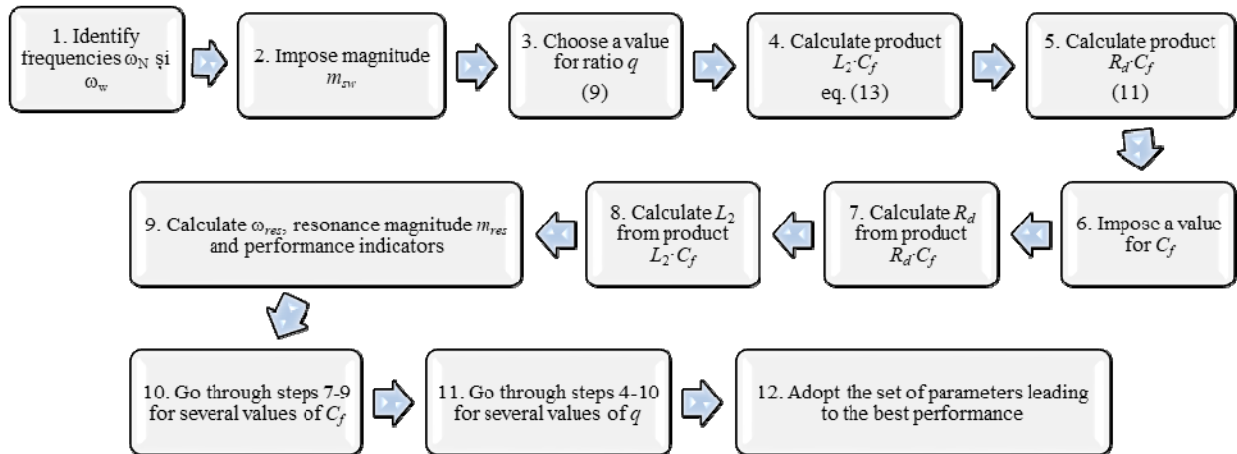
As shown in Fig. 12, during the operation in traction regime of the active substation, the currents drawn by the traction transformer from the power supply are distorted. The total harmonic distortion factor is of about 12 %, and the main harmonics are of orders 11, 13, 23 and 25 (Fig. 13).

When set 1 of parameters is adopted for the LCL filter, the waveforms of input and output currents of the LCL filter show that the filter fulfills its mission to significantly reduce the switching effect (Fig. 14 and Fig. 15).
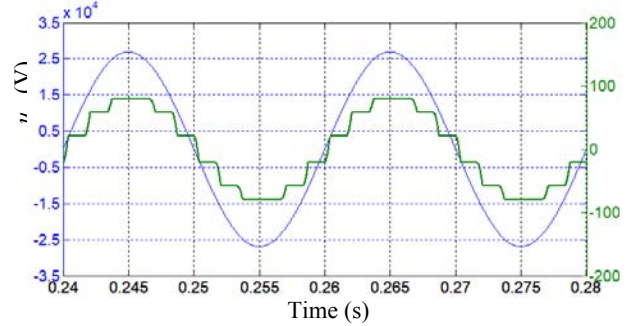

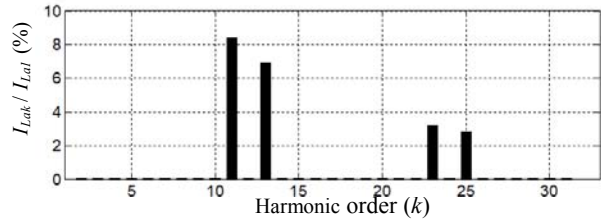Fig. 12. Phase voltage and current in traction regime.

Fig. 13. Harmonic spectrum of the current in the traction transformer primary, during the traction regime.
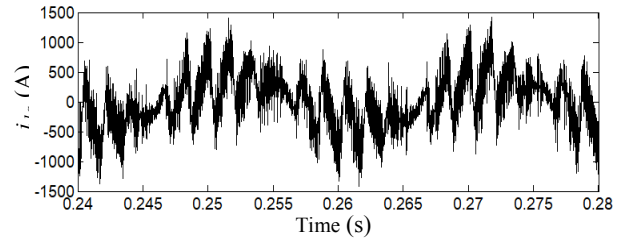

Fig. 14. Waveform of the LCL filter's input current for set 1 of parameters.

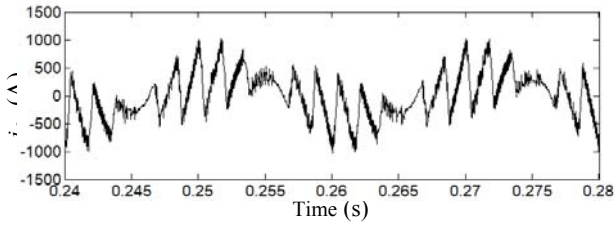Fig. 11. The algorithm for the design of the LCL filter with damping resistance.

Fig. 15. Waveform of the LCL filter's output current for set 1 of parameters.

As effect of a proper current injection in PCC through the LCL filter, the compensated current drawn from the power grid is almost sinusoidal (*THD*=3.45%) and nearly unity power factor is obtained (Fig. 16). The harmonic spectrum of the grid current shows that the main harmonics of orders 11, 13, 23 and 25 are all bellow 1% of the fundamental component (Fig. 17).

Good quality of the grid current (*THD*=4.95%) is illustrated too in Fig. 18, during the operation in regeneration mode. All harmonics in the range of 2 to 31 order are all bellow 0.65 % of the fundamental component (Fig. 19).

When the second set of parameters for the LCL filter is used in simulation, the waveforms in Fig. 20 and Fig. 21 show that the switching harmonics are only rejected to a small extent, resulting in a remaining harmonic distortion of about 8.85%.
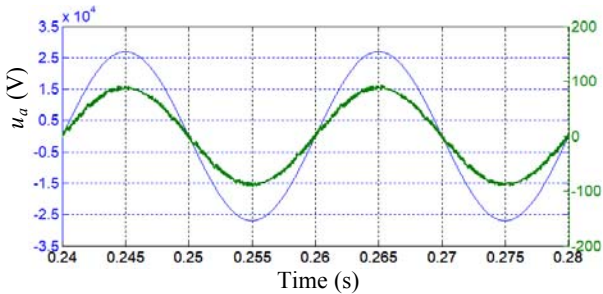

Fig. 16. Phase voltage and current upstream PCC in traction regime, for set 1 of parameters.
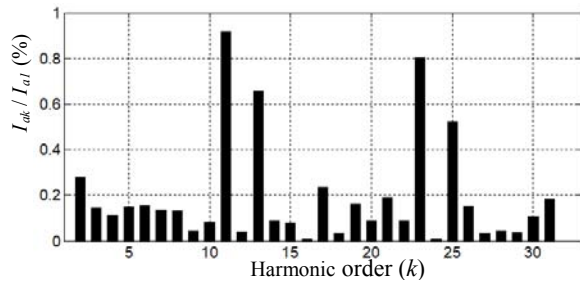

Fig. 17. Harmonic spectrum of the current upstream PCC, during the traction regime, for set 1 of parameters.
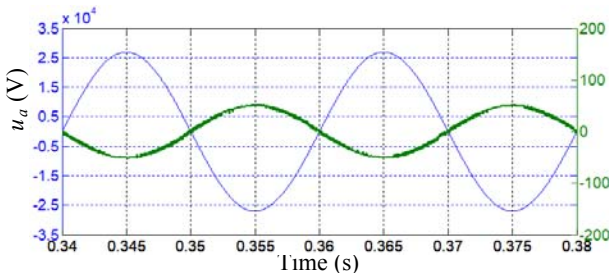

Fig. 18. Phase voltage and current upstream PCC regeneration regime, for set 1 of parameters.
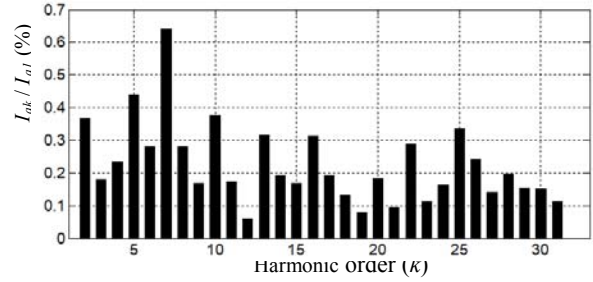

Fig. 19. Harmonic spectrum of the current upstream PCC, during the regeneration regime, for set 1 of parameters.
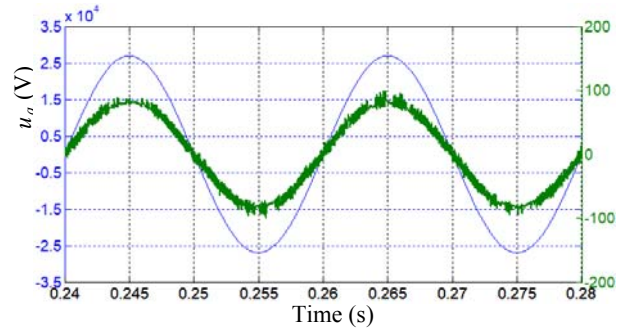

Fig. 20. Phase voltage and current upstream PCC in traction regime, for set 2 of parameters.
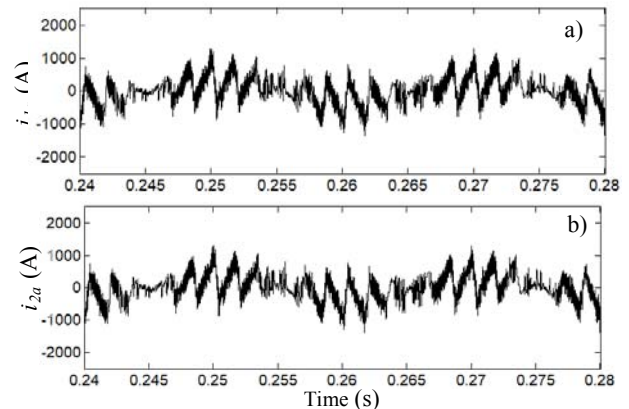

Fig. 21. Waveform of the LCL filter's input (a) and output (b) currents for set 2 of parameters.

As expected, the situation is even worse in the case of the third set of parameters (Fig. 22 and Fig. 23).

The global harmonic distortion of the compensated current is higher (*THD*=14.9%) and Fig. 23 illustrates the distorted compensating current provided by the LCL filter.
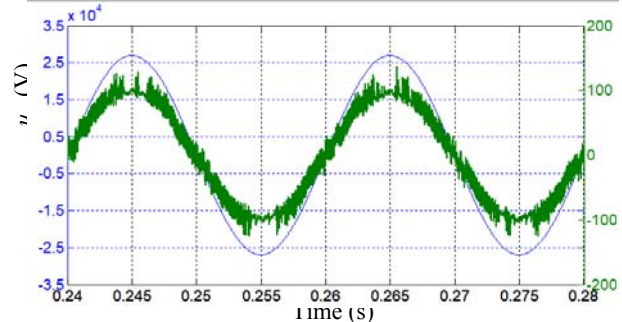

Fig. 22. Phase voltage and current upstream PCC in traction regime, for set 3 of parameters.
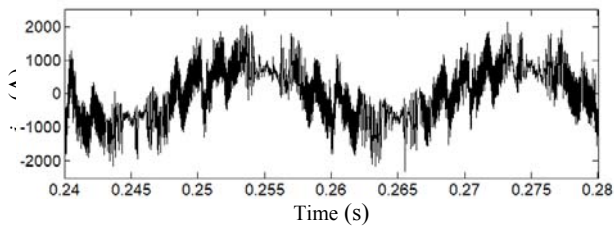
Fig. 15. Waveform of the LCL filter's output current for set 3 of parameters.

VII. Conclusions

This paper presents a method of designing a LCL filter with damping resistance for the connection of a three phase shunt active power filter to the power grid.

The algorithm is based on the imposition of the attenuation at the switching frequency and the imposition of the resonance frequency.

The performance indicators take into account the power losses on the damping resistors and the extent to which the harmonics to be compensated are influenced by the coupling filter.

The design algorithm is applied to the coupling filter used in an active DC-traction substation with 12-pulse parallel diode rectifier. Simulation results validate the theoretical achievements.

The proposed design algorithm for the coupling LCL filter can be also used in other active filtering applications, specifying that the load particularities (mainly through the values of f_N and f_{sw}) may lead to performances different from those outlined in this paper.

References

[1] M. E. Vilberger, A. V. Kulekina, and P. A. Bakholdin, "The twelfth-pulse rectifier for traction substations of electric transport," *IOP Conf. Series: Earth and Environmental Science*, no. 87, 2017, pp. 1–5.

[2] W. Brociek, R.Wilanowicz, and S. Filipowicz, "Cooperation of 12-pulse converter with a power system in dynamic state," *Przegląd Elektrotechniczny*, no. 5, 2014, pp. 67–70.

[3] C. Mayet, P. Delarue, A. Bouscayrol, E. Chattot, and J. N. Verhille, "Dynamic model and causal description of a traction power substation based on 6-pulse diode rectifier," 2014, in *Proc. IEEE Vehicle Power and Propulsion Conference (VPPC)*, 2014, pp. 1-6.

[4] T. Bałkowiec and W. Koczara, "Three-phase rectifier dedicated to DC traction substation," *Przegląd Elektrotechniczny*, no. 9, 2017, pp. 41-45.

[5] IEEE recommended practice and requirements for harmonic control in electrical power systems, *IEEE Std. 519-1992*.

[6] N. Gunavardhini and M. Chandrasekaran, "Power quality conditioners for railway traction - A review," *Automatika*, vol. 57, no. 1, pp. 150–162, 2016.

[7] W. Hosny, H.-E. Park, and J.-H. Song, "Investigation of shunt active power filters in railway systems, substation installation," *Journal of Energy and Power Engineering*, pp. 1974–1979, Oct. 2013.

[8] Y. Tang, P. C. Loh, P. Wang, F. H.Choo, F. Gao, and F. Blaabjerg, "Generalized design of high performance shunt active power filter with output LCL filter," *IEEE Trans. Ind. Electron.*, vol. 59, no. 3, pp. 1443-1452, March 2012.

[9] Q. Liu, L. Peng, Y. Kang, S. Tang, D. Wu, and Y. Qi, "A novel design and optimization method of an LCL filter for a shunt active power filter," *IEEE Trans. Ind. Electron.*, vol. 61, no. 8, pp. 4000-4010, Aug. 2014.

[10] C. H. Bae, M. S. Han, Y. K.Kim, and C. Y. Choi, "Simulation study of regenerative inverter for DC traction substation," in *Proc. ICEMS 2005*, vol. 2, Sept. 2005, pp. 1452-1456.

[11] . S. J. Jang, C. Y. Choi, C. H. Bae, S. H. Song, and C. Y. Won, "Study of regeneration power control inverter for DC traction with active power filter ability", in *Proc. 31st Annual Conference of IEEE*, Nov. 2005.

[12] J. M. Ortega, H. Ibaiondo, and A. Romo, "Kinetic energy recovery on railway systems with feedback to the grid," in *Proc. 9th World Congress on Railway Research*, May 22–26, 2011.

[13] J. M. Ortega, "Ingeber system for kinetic energy recovery & Metro Bilbao experience," in *Rail Techn. Forum Internat.*, Madrid, June 2011.

[14] Y. Warin, R. Lanselle, and M. Thiounn, "Active substation," in *Proc. World Congress on Railway Research*, Lille, France, May 2011.

[15] M. Popescu, A. Bitoleanu, V. Suru, and A. Preda, "System for converting the DC traction substations into active substations," in *Proc. ATEE 2015*, pp. 632–637, May 2015.

[16] X. Wang, F. Blaabjerg, and P. C. Loh, "Grid-Current-Feedback Active Damping for LCL Resonance in Grid-Connected Voltage Source Converters," *IEEE Trans. Power Electron.*, vol. 31, pp. 213-223, 2016.

[17] K.-B. Park, F. Kieferndorf, U. Drofenik, S. Pettersson, and F. Canales, "Weight minimization of LCL filters for high power converters," ," in *Proc. ECCE Asia 2015*, pp. 142–149, June 2015.

[18] W. Wu, Y. Liu, Y. He, H. S.-H. Chung, M. Liserre, and F. Blaabjerg, "Damping methods for resonances caused by LCL-filter-based current-controlled grid-tied power inverters: an overview," *IEEE Trans. Ind. Electron.*, vol. 64, no. 9, pp. 7402-7413, Sept. 2017.

[19] M. Popescu, A. Bitoleanu, and V. Suru, "On the design of LCL filter with passive damping in three-phase shunt active power filters," in *Proc. SPEEDAM 2016*, pp. 826-831, June 2016.

[20] A. Bitoleanu, M. Popescu, and M. Linca, "Limitations of LCL filter for three-phase shunt active power filters in active traction substations", in *Proc. SPEEDAM 2016*, pp. 671-676, June 2016.

[21] M. Popescu, A. Bitoleanu, and M. Dobriceanu, "Investigations on the Coupling LCL Filter in active traction substations," in *Proc. OPTIM-ACEMP 2017*, pp.654-659, May 2017.

[22] M. Popescu, A. Bitoleanu, and A. Preda, "A new design method of an LCL filter applied in active DC-traction substations," *IEEE Trans. Ind. Appl.*, vol. 54, issue 4, pp. 3497-3507, July/Aug. 2018.

[23] M. Popescu, A. Bitoleanu, M. Dobriceanu, and F. A. Teodorescu, "On the AC-connecting of a system for active filtering and regeneration in active DC-traction substations," in *Proc. ICATE 2018*, Oct. 2018.

[24] A. Bitoleanu, M. Popescu, and V. Suru, "Optimal controllers design in indirect current control system of active DC-traction substation," in *Proc. PEMC 2016*, pp. 904-909, Sept. 2016.

[25] A. Bitoleanu, M. Popescu, and C. V. Suru, "Theoretical and experimental evaluation of the indirect current control in active filtering and regeneration Systems," in Proc. OPTIM-ACEMP 2017, pp.759-764, May 2017.